LETTER

Tracking freshwater browning and coastal water darkening from boreal forests to the Arctic Ocean

Anders Frugård Opdal [1]* Tom Andersen,[2] Dag O. Hessen,[2] Christian Lindemann,[1] Dag L. Aksnes [1]
[1]Department of Biological Sciences, University of Bergen, Bergen, Norway; [2]Department of Biosciences, University of Oslo, Oslo, Norway

Scientific Significance Statement

Changes in land use, afforestation, reduced acidification, and climate are causing increased terrestrial primary production and vegetation density in the boreal zone. This greening on land contributes to increased exports of natural organic matter that have made inland waters become browner. The brown freshwater ultimately drains to the coast, but the impact on coastal waters is poorly understood. Here, we provide evidence that terrestrial greening and freshwater browning around the Baltic and North Sea has ramifications for coastal water clarity across thousands of kilometers, pointing toward an ecosystem connectivity from the Baltic lakes and forests to the Barents Sea.

Abstract

The forest cover of Northern Europe has been steadily expanding during the last 120 years. More terrestrial vegetation and carbon fixation leads to more export to surface waters. This may cause freshwater browning, as more degraded plant-litter ends up as chromophoric (colored) dissolved organic matter. Although most freshwater ultimately drains to coastal waters, the link between freshwater browning and coastal water darkening is poorly understood. Here, we explore this relationship through a combination of centennial records of forest cover and coastal water clarity, contemporary optical measurements in lakes and coastal waters, as well as an ocean drift model. We suggest a link between forest cover in Northern Europe and coastal water clarity in the Baltic, Kattegat, and Skagerrak Sea and show how brown-colored freshwater from Northern European catchments can dictate coastal water clarity across thousands of kilometers, from the Baltic lakes to the Barents Sea.

In many boreal and alpine areas, the trend in land use over the last century is less grazing and agriculture, and more forest cover and vegetation—a long-term greening process (Guay et al. 2014; Fuchs et al. 2015; Meyer-Jacob et al. 2015). In recent years, increased temperatures, CO_2 concentrations, nitrogen deposition, and precipitation has led to a longer

---

growing season (Barichivich et al. 2013), more vegetation (Myneni et al. 1997) and forest growth (Thomas et al. 2010; Høgberg et al. 2017). For instance, the growing stock of Fennoscandian forests (Norway, Sweden, and Finland) has more than doubled during the last century (Claesson et al. 2015; Breidenbach et al. 2020; Anon 2022), partly also due to large forest planting and management programs started in the 1950s (Östlund et al. 1997).

Higher terrestrial plant biomass and primary production adds dissolved organic carbon (DOC) to water, either directly by leachate from litterfall or roots with associated mycorrhiza, or indirectly via bogs and soils. This is the dominant pool of carbon in most freshwaters in the boreal zone (Cole et al. 2007), where it is visible as a yellow or brown color, often referred to as chromophoric (colored) dissolved organic matter (CDOM). The greening of catchments therefore has a profound browning effect on recipient freshwaters (Meyer-Jacob et al. 2015; Finstad et al. 2016; Kritzberg 2017; Skerlep et al. 2020), which in turn drain to marine coastal waters. Changed hydrology (de Wit et al. 2016), peatland ditching (Nieminen et al. 2021), and reduced acid deposition (Evans et al. 2006; Monteith et al. 2007) will also contribute to this browning.

In a study of 77 Swedish and Norwegian freshwater lakes, CDOM was found to be the main driver of light attenuation, even in highly eutrophic lakes (Thrane et al. 2014). In the Baltic Sea, which supplies around 70% of the freshwater to the southern part (Skagerrak) of the Norwegian Coastal Water (NCW; Aure et al. 1998), CDOM from freshwater sources is an important driver of light attenuation (Kowalczuk et al. 2006). Here, changes in chlorophyll *a* (Chl *a*) concentration typically explains maximum 10–17% of the variation in water clarity (Fleming-Lehtinen and Laamanen 2012; Harvey et al. 2019), while CDOM can account for up to 70–90% of that variation (Kowalczuk et al. 2006; Harvey et al. 2019). The importance of Chl *a* concentration for light attenuation is highest during periods of low freshwater discharge and high biological activity (Kowalczuk et al. 2006; Fleming-Lehtinen and Laamanen 2012).

For the North Sea, Skagerrak Sea, and Baltic Sea, several studies have found that light attenuation has been increasing throughout the 20th century (Sandén and Håkansson 1996; Aarup 2002; Dupont and Aksnes 2013; Capuzzo et al. 2015; Opdal et al. 2019; Kahru et al. 2022), inferred from a gradual decreasing Secchi disk depth—a phenomenon often referred to as coastal water darkening. Interestingly, the term darkening originally referred to the freshening of coastal waters, and associated increase in light attenuation (Aksnes et al. 2009), but is more commonly used as any nonbiotic driver of reduced light penetration in coastal waters, including both dissolved and suspended matter (Frigstad et al. 2013; McGovern et al. 2019; Blain et al. 2021; Konik et al. 2021).

There is little evidence that increasing Chl *a* concentration has been an important driver of coastal water darkening in these areas (Fleming-Lehtinen and Laamanen 2012; Opdal et al. 2019; Kahru et al. 2022), but *see* Sandén and Håkansson (1996) for a general discussion. Rather, increasing CDOM concentration from freshwater sources has been suggested as a likely cause (Fleming-Lehtinen and Laamanen 2012; Dupont and Aksnes 2013; Opdal et al. 2019; Kahru et al. 2022), and possibly also wind driven resuspension of sediments—at least for the most recent decades and in the shallower parts of the North Sea (Capuzzo et al. 2015; Wilson and Heath 2019).

In this study, we investigate the terrestrial and freshwater drivers of 120 years of coastal water darkening in the Skagerrak Sea and explore its extended geographical impact on light attenuation along 3000 km of Norwegian coastline.

Materials and methods

See Table 1 for a list of abbreviations, units and explanations, and Opdal (2022) for all raw data used in this study.

Estimation of nonphytoplankton light attenuation in the Skagerrak Sea

Nonphytoplankton light attenuation (K_{NON}) from substances such as suspended and dissolved organic matter was estimated based on a combination of in situ measurements of Secchi disk depth (S, m, $N = 256,536$), salinity (SAL, psu, $N = 714,400$), and Chl *a* (CHL, mg m^{-3}, $N = 943,548$, includes 6944 estimates from cell counts and phytoplankton color index; *see* table S1) taken in the Baltic, Kattegat, and Skagerrak seas between 1903 and 2021 (Supporting Information Table S1; Fig. S2). As the focus of this study is largely on the freshwater endmember of coastal waters, we represent salinity (SAL) as the freshwater fraction, FWf $= 1 -$ SAL/35.2, where 35.2 is the salinity of the assumed ocean endmember, North Atlantic Water (Aksnes 2015).

Due to variable data coverage, we applied two separate approaches (*A1970* and *A1903*) for estimating K_{NON}. Both approaches rely on the mechanistically derived relationship between Secchi disk depth (S) and the attenuation coefficient of downwelling irradiance, $K_S = 1.48/S$ (Lee et al. 2018). For a general discussion, see Turner et al. (2022).

The first approach (*A1970*) is based on a single generalized additive model that incorporates 48,143 simultaneous (same day and location) measurements of Secchi disk depth (S), salinity (SAL) and Chl *a* (CHL), such that

$$S = s_1(SAL, CHL) + s_2(YEAR) + \epsilon \tag{1}$$

where s_1 and s_2 are smoothing terms and ε is the error term. Low spatiotemporal coverage before 1970 limited this approach to the years 1970–2021. However, it allowed us to disentangle the effects of salinity (SAL) and Chl *a* (CHL) on light attenuation (K_S) as well as predicting the annual (1970–2021) change in K_{NON} for a fixed value of SAL and CHL. See the Supporting Information for model details.

The second approach (*A1903*) covered the period 1903–2021 and follows the methodology described in Opdal et al. (2019). For photosynthetically active radiation (400–700 nm)

Table 1. Abbreviations, explanations, and units.

Abbr.	Explanation	Unit	Comment
NCW	Norwegian coastal water		
NCC	Norwegian coastal current		Transports NCW along the coast
CDOM	Color dissolved organic matter		
DOC	Dissolved organic carbon		
SAL	Salinity	psu	
FWf	Freshwater fraction		$FWf = 1 - SAL/35.2$
S	Secchi disk depth	m	
CHL	Chl a concentration	mg m^{-3}	
K_S	Light attenuation derived from S	m^{-1}	$K_S = 1.48/S$ (Lee et al. 2018)
K_{PHY}	Light attenuation from CHL	m^{-1}	$K_{PHY} = 0.121$ CHL$^{0.428}$ (Morel 1988)
K_W	Light attenuation from water	m^{-1}	0.0089 m^{-1} (Morel and Maritorena 2001)
K_{NON}	Nonphytoplankton light attenuation	m^{-1}	$K_{NON} = K_S - K_{PHY} - K_W$ (Eq. 2)
$K_{FW\ NON}$	K_{NON} of the freshwater endmember	m^{-1}	FWf = 1
tot	Total reduction in $K_{FW\ NON}$ with distance	m^{-1} km^{-1}	tot = deg + fwr
deg	Reduction in $K_{FW\ NON}$ caused by degradation	m^{-1} km^{-1}	
fwr	Reduction in $K_{FW\ NON}$ caused by freshwater replacement	m^{-1} km^{-1}	
A_i	Drainage areas from Skagerrak (A_0) to the Barents Sea (A_6)		
FW_i	Freshwater discharge from A_i	m^3 s^{-1}	

we assumed that light attenuation from sources other than phytoplankton and water itself (K_{NON}) can be derived from a quasi-inherent composite light attenuation, such that

$$K_{NON} = K_S - K_{PHY} - K_W \qquad (2)$$

where K_{PHY} is the light attenuation from phytoplankton ($K_{PHY} = 0.121$ CHL$^{0.428}$, m^{-1}; Morel 1988) and K_W is the contribution of water itself ($K_W = 0.0089$ m^{-1}, Morel and Maritorena 2001). Based on 84,719 pairs of Secchi disk and salinity measurements and 943,548 Chl a measurements and estimates (Supporting Information Fig. S2G–I), we constructed two separate generalized additive models (Supporting Information Eqs. S1, S2) that allowed us to obtain annual estimates of Secchi disk depth (S, Supporting Information Eq. S1) and Chl a (CHL, Supporting Information Eq. S2), and their respective light attenuation coefficients K_S and K_{PHY}, from 1903 to 2021 in the southern part of the NCW in the Skagerrak Sea (LAT = 58°N, LON = 8.5°E, star in Fig. 1) in January (MONTH = 1), when the effect of Chl a is at its lowest.

Connecting coastal water darkening to freshwater browning

Coastal water darkening in the southern part of the NCW, as expressed by increased K_{NON}, was linked to freshwater browning through the nonchlorophyll light attenuation of the freshwater endmember of the coastal water ($K_{FW\ NON}$).

In the first approach (*A1970*, YEAR = 1970–2021), a general estimate of $K_{FW\ NON}$ was obtained from Eq. 1 by setting Chl a and salinity both to zero, such that $K_{FW\ NON}$(YEAR) = K_S(YEAR, SAL = 0, CHL = 0). In the second approach (*A1903*, YEAR = 1903–2021), $K_{FW\ NON}$ was derived for the southern NCW in January from Eq. 2, where K_S is obtained from Secchi disk depth (S) at zero salinity (Supporting Information Eq. S1), such that $K_{FW\ NON}$(YEAR) = K_S(YEAR, LAT = 58, LON = 8.5, MONTH = 1, SAL = 0) – K_{PHY}(YEAR, LAT = 58, LON = 8.5, MONTH = 1) – K_W. An increase in $K_{FW\ NON}$ over time indicates that the freshwater entering the coastal water has undergone browning. The latter estimate of $K_{FW\ NON}$ was then compared to the change in forest cover (*see* Supporting Information) in the relevant drainage area (Fig. 1).

Reduced $K_{FW\ NON}$ from the Skagerrak to the Barents Sea

The freshwater endmember of the southern NCW originates from rivers draining into the Kattegat and Baltic Sea ($\sim$ 15,000 m^3 s^{-1}), North Sea ($\sim$ 4500 m^3 s^{-1}), and Skagerrak ($\sim$ 2500 m^3 s^{-1}), making up a total of ca 22,000 m^3 freshwater per second (Aure et al. 1998). From Skagerrak, the NCW is transported northwards by the Norwegian Coastal Current (NCC; Sætre 2007).

A reduction in $K_{FW\ NON}$ in the NCW downstream from Skagerrak, is expected according to two processes. The first is CDOM degradation caused by bacterial consumption and
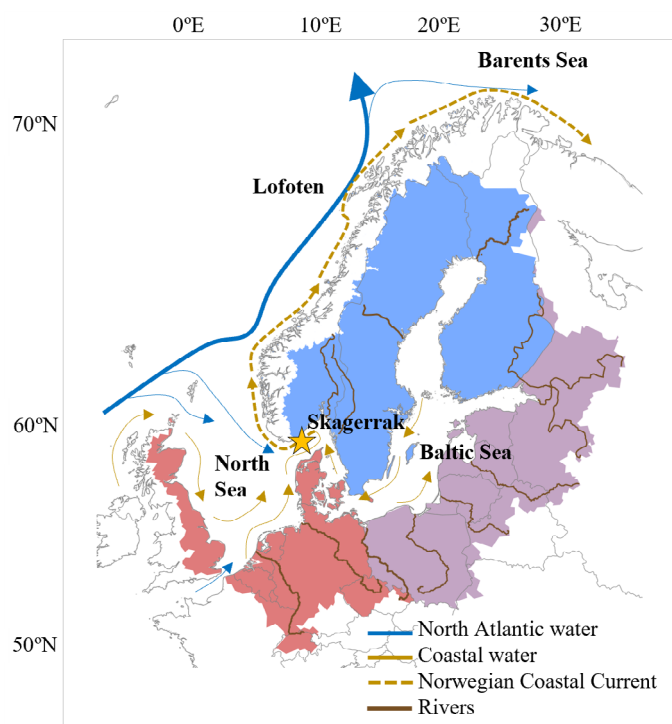
Fig. 1. Overview of drainage area, major rivers, water masses and currents. Drainage areas to the Skagerrak, Baltic Sea and North Sea are divided into three regions: Fennoscandia (blue), North-eastern Europe (purple), and North-western Europe (red). Rivers from the largest watersheds are drawn in dark brown, while ocean current trajectories supplying Atlantic and coastal water masses are denoted with blue and brown arrows, respectively. Dashed thick line show the Norwegian Coastal Current transporting coastal water along the Norwegian coast. The star denotes the geographical location in the southern part of the Norwegian Coastal Water (Skagerrak Sea), where we have estimated the nonphytoplankton light attenuation for the years 1903–2021.

photo oxidation/degradation (Fransner et al. 2016; Massicotte et al. 2017). The second is freshwater drainage to the NCW from additional sources along the western Norwegian coast. Because western Norwegian drainage areas are less vegetated and more alpine than those further east, the light attenuation from these freshwaters will be lower (cf. Thrane et al. 2014). Hence, we expect that the NCW freshwater endmember will gradually be more influenced by the clearer freshwater of western Norwegian origin than that of Baltic origin, as distance from the Skagerrak increases (referred to as replacement effect below).

Although the effect of CDOM degradation rate on $K_{FW\ NON}$ (deg, $m^{-1}\ km^{-1}$) downstream the NCC is unknown, we estimate the freshwater replacement effect (fwr, $m^{-1}\ km^{-1}$) from information on the discharge ($m^3\ s^{-1}$) and light attenuation (m^{-1}) of the added freshwater along the coast (*see* below). In a previous study (Aksnes 2015; *see* Supporting Information), the total reduction in $K_{FW\ NON}$ with distance was estimated, tot = 0.058 $m^{-1}\ km^{-1}$. Thus, the effect from CDOM

degradation, deg, can be inferred from the difference, deg = tot – fwr. Knowing deg and the NCC transportation speed (*see* below) of a CDOM molecule ($km\ d^{-1}$) provides an estimate of the CDOM degradation rate ($m^{-1}\ d^{-1}$).

Freshwater replacement effect on $K_{FW\ NON}$

The mean winter (December–February, 1990–2020) freshwater discharge (FW, $m^3\ s^{-1}$) into the NCW was retrieved for six drainage regions (A_1 to A_6) between Skagerrak and the Barents Sea (*see* Supporting Information). The corresponding nonchlorophyll light attenuation of this freshwater was drawn from measurements taken in 2011 in 13 lakes draining to the Western Norwegian coastline (Supporting Information Fig. S6; Thrane et al. 2014). Starting in Skagerrak (A_0) we then obtained updated estimates of $K_{FW\ NON}$ for each additional drainage area (A_i) using the fraction (f_i) between the freshwater of Skagerrak (Baltic) origin ($FW(A_0) = 22,000\ m^3\ s^{-1}$) and the added freshwater from the respective drainage areas along the western Norwegian coast ($FW(A_i)$, $m^3\ s^{-1}$)

$$K_{FW\ NON}(A_i) = f_i \cdot K_{FW\ NON}(A_0) + (1 - f_i) \cdot K_{FW\ NON}(Lakes) \quad (3)$$

where

$$f_i = \frac{FW(A_0)}{\sum_{i=0}^{i} FW(A_i)} \quad (4)$$

Transport and retention of a CDOM molecule

The drift trajectory and speed of 100,000 neutrally buoyant virtual CDOM molecules from the Skagerrak to the Barents Sea, was estimated according to advection and turbulent diffusivity, using a Lagrangian particle tracking model in the Python-based framework OpenDrift (Dagestad et al. 2018). See Supporting Information for details.

Results and discussion

Overall, we found that variation in Secchi disk depth (S) was adequately described by a statistical model including Chl a, salinity, and year (*A1970*, Eq. 1; Fig. 2; Supporting Information Fig. S3). The relationship between the light attenuation coefficient and Chl a concentration (Fig. 2C), is close to the general function $K_{PHY} = 0.121 \cdot CHL^{0.428}$ derived by Morel (1988). This adds confidence to approach *A1903* (Eq. 2), where K_{PHY} is derived directly from CHL (Supporting Information Eq. S2) using this function. Also, the relationship between light attenuation and the freshwater fraction (Fig. 2D), resembles the functional form described by Højerslev et al. (1996) for CDOM light absorption $a(380)$, suggesting the model captures some fundamental mechanisms of light attenuation in the region. An apparent increase in light attenuation (0.8–1.1 m^{-1}) of the nonphytoplankton freshwater endmember (Fig. 2E) from 1970 to 2020, could
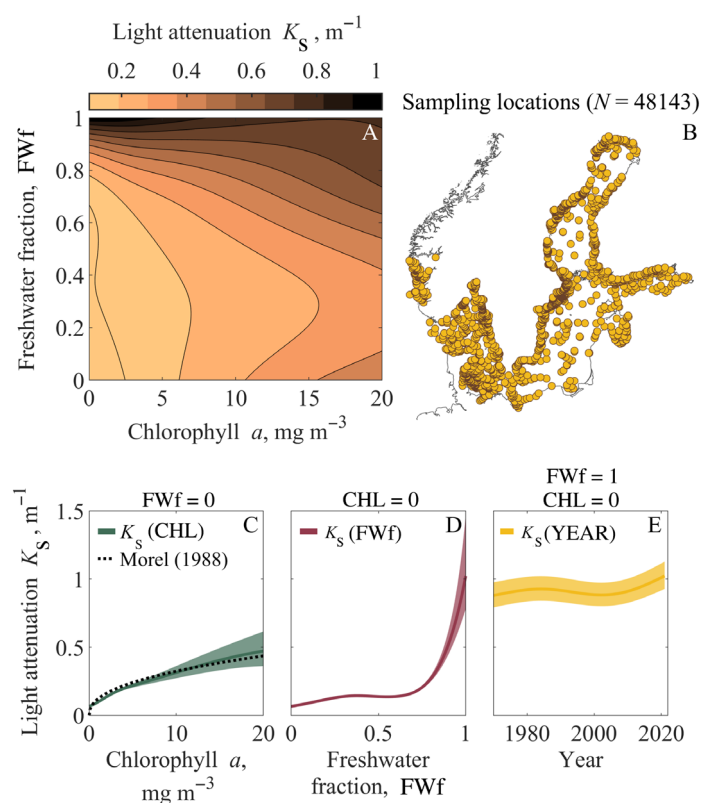
Fig. 2. Effect of Chl *a*, freshwater, and time on light attenuation from predictions of model approach *A1970* (Eq. 1) covering the years 1970–2021. The overall model explained 39% of the deviance ($N = 48{,}143$ and p-value <0.001). (**A**) How light attenuation (K_S) relates to Chl *a* concentration (CHL) and freshwater fraction (FWf); (**B**) the location of the samples; (**C**) the relationship between K_S and CHL, in the absence of freshwater (FWf = 0) in 2021. Overlaid is the general relationship, $K_{PHY} = 0.121 \cdot CHL^{0.428}$, derived by Morel (1988) and used in *A1903* (Eq. 2). A simple linear regression between our modeled K_S (CHL) and the K_{PHY} from Morel (1988), $K_{PHY} \sim K_S$ (CHL) $\alpha + \beta$, gives an $R^2 = 0.98$ ($\alpha = 1.03 \pm 0.03$ 95% CI and $\beta = 0.01 \pm 0.006$ 95% CI). (**D**) The influence of freshwater (FWf) on K_S at zero CHL in 2021; (**E**) the change in the nonphytoplankton light attenuation of the freshwater endmember, $K_{FW \, NON}$ (CHL = 0, FWf = 1). See also Supporting Information Fig. S4 for a detailed comparison between the model predictions and observations.

indicate increasing CDOM concentrations in freshwater sources.

During the period 1900 to 2020 the net forest cover in the region increased by around 200,000 km², or by ca 25% (Fig. 3A; Supporting Information Fig. S1). Most of this increase (~ 70%) stem from Fennoscandia (Supporting Information Fig. S1). Over the same period (1903–2021, *A1903*), we found an increase in the light attenuation, K_S, of the southern NCW (Supporting Information Fig. S4A), unrelated to Chl *a* concentration (Supporting Information Fig. S4A), even at low freshwater fractions. Model A1903 thus suggests a centennial increase in the nonphytoplankton light attenuation of the freshwater endmember in the southern NCW, $K_{FW \, NON}$, from 0.6 to 1.4 m⁻¹ (Fig. 3B). This increase was significantly
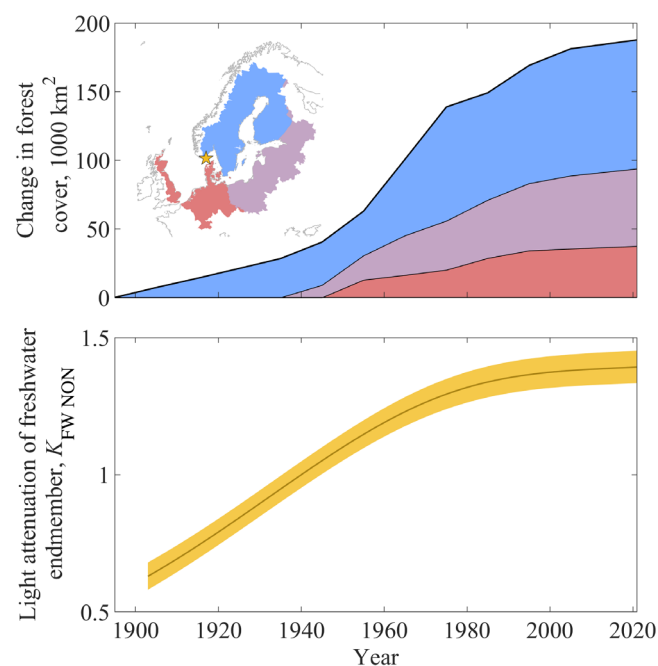

Fig. 3. Northern European forest cover and the nonphytoplankton light attenuation of the freshwater endmember ($K_{FW \, NON}$) of the Norwegian Coastal Water. (**A**) The increase in the forest cover (1000 km²) of catchment areas draining to the Baltic Sea, North Sea, and Skagerrak in the period 1900–2020. Colors correspond to the geographical areas in the map insert (Fig. 1). (**B**) The estimate (and 95% CI) of nonphytoplankton light attenuation of the freshwater fraction ($K_{FW \, NON}$) of the Skagerrak Sea (star in map insert) for the period 1903–2021 using the approach *A1903* (Eq. 2). A simple linear regression between forest cover in the Baltic Sea and North Sea drainage area (FC) and $K_{FW \, NON}$ in the southern NCW, $K_{FW} \sim \alpha$ FC $+ \beta$, gives an $R^2 = 0.90$ ($\alpha = 0.0034$ m⁻¹ 1,000 km⁻² $\pm 3 \times 10^{-4}$ 95% CI, $N = 13$).

larger than the seasonal variations in light attenuation (Supporting Information Fig. S4D,E). The model-estimate of $K_{FW \, NON}$ for the year 2008 (1.38 ± 0.06 95% CI) was close to that estimated (for 440 nm) by Aksnes (2015) in the same year (1.47 ± 0.24 95% CI), supporting our model estimate. The increase in $K_{FW \, NON}$ (Fig. 3B) and its apparent association with forest cover (Fig. 3A) corresponds well to a series of studies suggesting that terrestrial primary production and vegetation coverage (greening) drive freshwater browning through increased concentrations of CDOM (Kritzberg 2017; Creed et al. 2018; Skerlep et al. 2020).

While ca 90% of the centennial forest increase in Europe stem from the conversion from grassland and cropland (Fuchs et al. 2015), some afforestation is also facilitated through peatland ditching which cause organic carbon leaching and freshwater browning (Nieminen et al. 2021; Williamson et al. 2021; Härkönen et al. 2023). Ditching also increases freshwater Fe concentrations (Estlander et al. 2021), further enhancing light absorption (Xiao et al. 2013; Weyhenmeyer et al. 2014). However, dissolved Fe is likely to have little impact on light attenuation in coastal waters, as around 95%
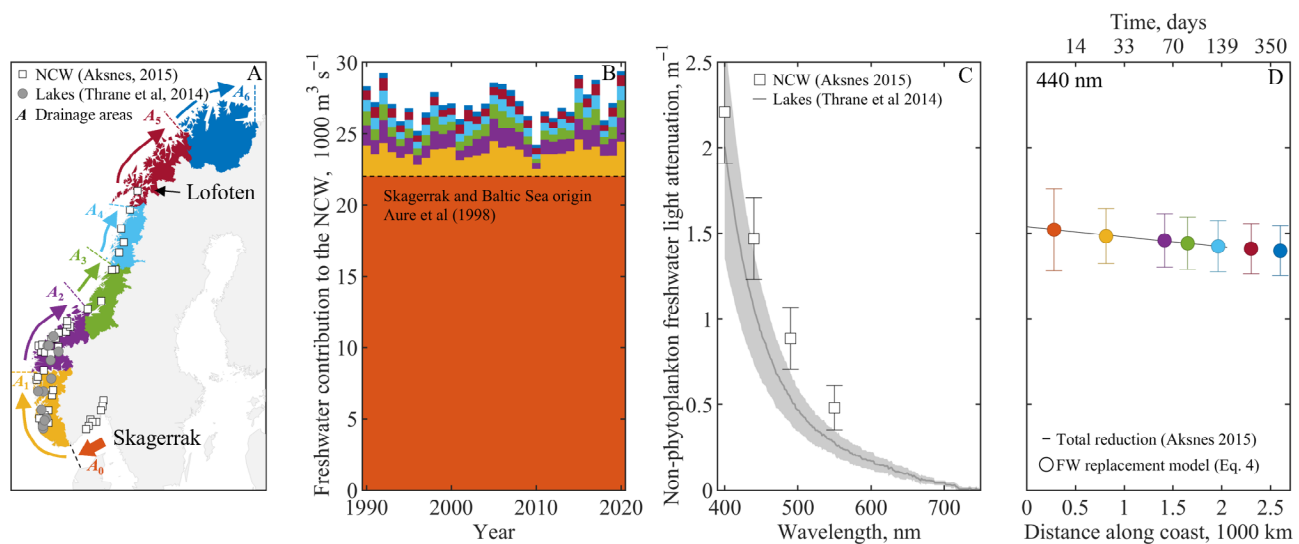
Fig. 4. Spatiotemporal persistence of the nonphytoplankton light attenuation of the freshwater endmember ($K_{FW\ NON}$) in the NCW. According to Aksnes (2015), the total reduction (tot) of $K_{FW\ NON}$ from Skagerrak to the Barents Sea was 0.058 m^{-1} 1,000 km^{-1} at 440 nm. This estimate was based on measurements from 40 locations downstream the NCC (**A**, squares). The freshwater replacement model (*see* Eq. 3) calculates the expected reduction (fwr), in $K_{FW\ NON}$ from the Skagerrak Sea (A_0, orange color) and northwards (arrows in **A**) based on the addition of new (clearer) freshwater from Western Norwegian drainage areas (A_1–A_6, **A,B**). Light attenuation of this added freshwater (shaded area in **C**) is the average of 13 Western Norwegian lakes (circles in **A**) measured by Thrane et al. (2014), and was below that of the NCW (squares in **C**). The freshwater replacement model (Eq. 3) predicts a reduction in $K_{FW\ NON}$ of 0.0575 m^{-1}1,000 km^{-1} (at 440 nm, shown as circles in **D**) which is very close to the total reduction estimated by Aksnes (2015). This suggests minor effect of CDOM degradation (deg) in the NCW. Also shown in the top *x*-axis in **D** is the mean transportation time of a CDOM molecule from the Skagerrak to the Barents Sea, based on the drift simulation model shown in Supporting Information Fig. S7.

is removed through flocculation during estuarine mixing (Sholkovitz 1976; Sholkovitz 1978). In comparison, flocculation only removes 3–16% of the DOC (Sholkovitz 1976; Asmala et al. 2014). Additional drivers of freshwater browning are changed hydrology (de Wit et al. 2016), and the reduction in atmospheric sulfur deposition (Evans et al. 2006; Monteith et al. 2007).

While $K_{FW\ NON}$ is clearly influenced by CDOM, wind driven resuspension of bottom sediments has also been suggested to decrease water clarity (Capuzzo et al. 2015; Wilson and Heath 2019). By selecting our location in the southern NCW, more than 20 km offshore and at a depth of 520 m, the effect of riverine borne or bottom resuspended particulate matter should be minimized (Opdal et al. 2019; Thewes et al. 2021). We also note that our models account for only 39% (Eq. 1; Supporting Information Fig. S3), 47% (Supporting Information Eq. S1; Fig. S4) and 36% (Supporting Information Eq. S2; Fig. S4) of the deviance in the observations, leaving ample room for additional sources of variation (*see* Supporting Information).

Having established a centennial change in the freshwater endmember in the southern NCW, mainly of Baltic origin (Aure et al. 1998), we then investigated how far this Baltic freshwater persist in the NCW. Results from two previous studies (Thrane et al. 2014; Aksnes 2015) suggest that the $K_{FW\ NON}$ of the NCW (Fig. 4C) was higher than the average of 13 Western Norwegian lakes (Fig. 4C; Supporting Information

Fig. S6). Even though measurements of light attenuation in the lakes are not directly transferable to those at the river outlet, the steep terrain, small watersheds, and short transit times in Western Norwegian catchments (Thrane et al. 2014), will likely minimize the discrepancy compared to other landscapes.

Along the Norwegian coast we found that a total decrease in $K_{FW\ NON}$, (0.058 m^{-1} 1000 km^{-1}, Aksnes 2015) could be explained by the freshwater replacement effect (0.0575 m^{-1} 1000 km^{-1}; Eq. 3). This suggests little or no degradation of CDOM between the southern NCW and Lofoten, and that the reduction in $K_{FW\ NON}$ over distance is due to increased influence of relatively clear freshwater from western Norwegian water sheds (Thrane et al. 2014). Most of the degradation of CDOM from microbial or photochemical oxidation happens in lakes and rivers, and within the first few months after entering the coastal waters (Vähätalo and Wetzel 2004; Timko et al. 2015; Allesson et al. 2021). This leaves more recalcitrant CDOM further away from the freshwater sources (Tranvik et al. 2009; Fransner et al. 2016; Massicotte et al. 2017), which in our case are mainly located around the Baltic Sea. A recent estimate suggests that 80% of the terrestrial DOC in the Baltic Sea is degraded before it reaches the Skagerrak (Fransner et al. 2016). In addition, we can assume an in situ production of new CDOM by marine phytoplankton accounting for up to 25% of the total CDOM (Yamashita and Tanoue 2004; Romera-Castillo et al. 2010). However, since centennial

phytoplankton concentrations in the NCW appeared unchanged (Supporting Information Fig. S4A), this should not affect the overall patterns described.

Moreover, we found that the transportation speed of a virtual CDOM molecule from Skagerrak to the Barents Sea is measured on the order of months (Supporting Information Fig. S7), rather than years and decades as in the Baltic Sea (Fransner et al. 2016). The median horizontal speed of a CDOM molecule was $0.11 \, \text{m s}^{-1}$, which is close to the reported average speed of the NCC (Sætre 2007). After 150 and 350 d, 50% of the molecules had reached the Lofoten and Barents Sea, respectively. Hence, the absence of a CDOM degradation effect could thus either be due to a recalcitrant fraction of CDOM (Fransner et al. 2016), or simply due to the short transportation time, or both.

In summary, we propose that a centennial increase in vegetation cover in Northern Europe has led to browner freshwaters due to increased CDOM concentrations. This browning and subsequent decrease in light attenuation is detectable downstream in the freshwater endmember of the NCW across several thousand kilometers. This connects the Barents Sea to the Baltic Sea, and possibly to the surrounding lakes and forests, pointing to an ecosystem connectivity from land to sea over great distances.

References

Aarup, T. 2002. Transparency of the North Sea and Baltic Sea—A Secchi depth data mining study. Oceanologia **44**: 323–337.

Aksnes, D. L. 2015. Sverdrup critical depth and the role of water clarity in Norwegian Coastal Water. ICES J. Mar. Sci. **72**: 2041–2050. doi:10.1093/icesjms/fsv029

Aksnes, D. L., N. Dupont, A. Staby, O. Fiksen, S. Kaartvedt, and J. Aure. 2009. Coastal water darkening and implications for mesopelagic regime shifts in Norwegian fjords. Mar. Ecol. Prog. Ser. **387**: 39–49. doi:10.3354/meps08120

Allesson, L., B. Koehler, J. E. Thrane, T. Andersen, and D. O. Hessen. 2021. The role of photomineralization for CO_2 emissions in boreal lakes along a gradient of dissolved organic matter. Limnol. Oceanogr. **66**: 158–170. doi:10.1002/lno.11594

Anon. 2022. The Finnish forest inventory. Available from https://www.luke.fi/en/statistics

Asmala, E., D. G. Bowers, R. Autio, H. Kaartokallio, and D. N. Thomas. 2014. Qualitative changes of riverine dissolved organic matter at low salinities due to flocculation. J. Geophys. Res. Biogeosci. **119**: 1919–1933. doi:10.1002/2014JG002722

Aure, J., D. Danielssen, and E. Svendsen. 1998. The origin of Skagerrak coastal water off Arendal in relation to variations in nutrient concentrations. ICES J. Mar. Sci. **55**: 610–619. doi:10.1006/jmsc.1998.0395

Barichivich, J., and others. 2013. Large-scale variations in the vegetation growing season and annual cycle of atmospheric CO_2 at high northern latitudes from 1950 to 2011. Glob. Chang. Biol. **19**: 3167–3183. doi:10.1111/gcb.12283

Blain, C. O., S. C. Hansen, and N. T. Shears. 2021. Coastal darkening substantially limits the contribution of kelp to coastal carbon cycles. Glob. Chang. Biol. **27**: 5547–5563. doi:10.1111/gcb.15837

Breidenbach, J., A. Granhus, G. Hylen, R. Eriksen, and R. Astrup. 2020. A century of National Forest Inventory in Norway—Informing past, present, and future decisions. For Ecosyst **7**: 46.

Capuzzo, E., D. Stephens, T. Silva, J. Barry, and R. M. Forster. 2015. Decrease in water clarity of the southern and central North Sea during the 20th century. Glob. Chang. Biol. **21**: 2206–2214. doi:10.1111/gcb.12854

Claesson, S., K. Duvemo, A. Lundström, and P.-E. Wikberg. 2015. *Skogliga konsekvensanalyser 2015—SKA 15*. Skogsstyrelsen Rapport 10.

Cole, J. J., and others. 2007. Plumbing the global carbon cycle: Integrating inland waters into the terrestrial carbon budget. Ecosystems **10**: 171–184. doi:10.1007/s10021-006-9013-8

Creed, I. F., and others. 2018. Global change-driven effects on dissolved organic matter composition: Implications for food webs of northern lakes. Glob. Chang. Biol. **24**: 3692–3714. doi:10.1111/gcb.14129

Dagestad, K. F., J. Röhrs, Ø. Breivik, and B. Ådlandsvik. 2018. OpenDrift v1.0: A generic framework for trajectory modelling. Geosci. Model Dev. **11**: 1405–1420. doi:10.5194/gmd-11-1405-2018

de Wit, H. A., and others. 2016. Current Browning of surface waters will Be further promoted by wetter climate. Environ. Sci. Technol. Lett. **3**: 430–435. doi:10.1021/acs.estlett.6b00396

Dupont, N., and D. L. Aksnes. 2013. Centennial changes in water clarity of the Baltic Sea and the North Sea. Estuar. Coast Shelf. S. **131**: 282–289. doi:10.1016/j.ecss.2013.08.010

Estlander, S., E. Pippingskold, and J. Horppila. 2021. Artificial ditching of catchments and brownification-connected water quality parameters of lakes. Water Res. **205**: 117674. doi:10.1016/j.watres.2021.117674

Evans, C. D., P. J. Chapman, J. M. Clark, D. T. Monteith, and M. S. Cresser. 2006. Alternative explanations for rising dissolved organic carbon export from organic soils. Glob. Chang. Biol. **12**: 2044–2053. doi:10.1111/j.1365-2486.2006.01241.x

Finstad, A. G., and others. 2016. From greening to browning: Catchment vegetation development and reduced S-deposition promote organic carbon load on decadal time scales in Nordic lakes. Sci. Rep. **6**: 31944. doi:10.1038/srep31944

Fleming-Lehtinen, V., and M. Laamanen. 2012. Long-term changes in Secchi depth and the role of phytoplankton in

explaining light attenuation in the Baltic Sea. Estuar. Coast. Shelf. S. **102**: 1–10. doi:10.1016/j.ecss.2012.02.015

Fransner, F., and others. 2016. Tracing terrestrial DOC in the Baltic SeaA 3-D model study. Global Biogeochem. Cycl. **30**: 134–148. doi:10.1002/2014GB005078

Frigstad, H., and others. 2013. Long-term trends in carbon, nutrients and stoichiometry in Norwegian coastal waters: Evidence of a regime shift. Prog. Oceanogr. **111**: 113–124. doi:10.1016/j.pocean.2013.01.006

Fuchs, R., M. Herold, P. H. Verburg, J. Clevers, and J. Eberle. 2015. Gross changes in reconstructions of historic land cover/use for Europe between 1900 and 2010. Glob. Chang. Biol. **21**: 299–313. doi:10.1111/gcb.12714

Guay, K. C., P. S. A. Beck, L. T. Berner, S. J. Goetz, A. Baccini, and W. Buermann. 2014. Vegetation productivity patterns at high northern latitudes: A multi-sensor satellite data assessment. Glob. Chang. Biol. **20**: 3147–3158. doi:10.1111/gcb.12647

Härkönen, L. H., A. Lepistö, S. Sarkkola, P. Kortelainen, and A. Räike. 2023. Reviewing peatland forestry: Implications and mitigation measures for freshwater ecosystem browning. For. Ecol. Manage. **531**: 120776. doi:10.1016/j.foreco.2023.120776

Harvey, E. T., J. Walve, A. Andersson, B. Karlson, and S. Kratzer. 2019. The effect of optical properties on secchi depth and implications for eutrophication management. Front. Mar. Sci. **5**: 496. doi:10.3389/fmars.2018.00496

Högberg, P., T. Nasholm, O. Franklin, and M. N. Högberg. 2017. Tamm review: On the nature of the nitrogen limitation to plant growth in Fennoscandian boreal forests. For. Ecol. Manage. **403**: 161–185. doi:10.1016/j.foreco.2017.04.045

Højerslev, N. K., N. Holt, and T. Aarup. 1996. Optical measurements in the North Sea-Baltic Sea transition zone 1. On the origin of the deep water in the Kattegat. Cont. Shelf Res. **16**: 1329–1342. doi:10.1016/0278-4343(95)00075-5

Kahru, M., H. Bittig, R. Elmgren, V. Fleming, Z. Lee, and G. Rehder. 2022. Baltic Sea transparency from ships and satellites: Centennial trends. Mar. Ecol. Prog. Ser. **697**: 1–13. doi:10.3354/meps14151

Konik, M., M. Darecki, A. K. Pavlov, S. Sagan, and P. Kowalczuk. 2021. Darkening of the Svalbard fjords waters observed with satellite ocean color imagery in 1997–2019. Front. Mar. Sci. **8**: 699318. doi:10.3389/fmars.2021.699318

Kowalczuk, P., C. A. Stedmon, and S. Markager. 2006. Modeling absorption by CDOM in the Baltic Sea from season, salinity and chlorophyll. Mar. Chem. **101**: 1–11. doi:10.1016/j.marchem.2005.12.005

Kritzberg, E. S. 2017. Centennial-long trends of lake browning show major effect of afforestation. Limnol. Oceanogr Lett. **2**: 105–112.

Lee, Z. P., S. L. Shang, K. P. Du, and J. W. Wei. 2018. Resolving the long-standing puzzles about the observed Secchi depth relationships. Limnol. Oceanogr. **63**: 2321–2336. doi:10.1002/lno.10940

Massicotte, P., E. Asmala, C. Stedmon, and S. Markager. 2017. Global distribution of dissolved organic matter along the aquatic continuum: Across rivers, lakes and oceans. Sci. Total Environ. **609**: 180–191. doi:10.1016/j.scitotenv.2017.07.076

McGovern, M., and others. 2019. Implications of coastal darkening for contaminant transport, bioavailability, and trophic transfer in northern coastal waters. Environ. Sci. Technol. **53**: 7180–7182. doi:10.1021/acs.est.9b03093

Meyer-Jacob, C., J. Tolu, C. Bigler, H. Yang, and R. Bindler. 2015. Early land use and centennial scale changes in lake-water organic carbon prior to contemporary monitoring. Proc. Natl. Acad. Sci. U.S.A. **112**: 6579–6584. doi:10.1073/pnas.1501505112

Monteith, D. T., and others. 2007. Dissolved organic carbon trends resulting from changes in atmospheric deposition chemistry. Nature **450**: 537–U539. doi:10.1038/nature06316

Morel, A. 1988. Optical modeling of the upper ocean in relation to its biogenous matter content (case-I waters). J. Geophys. Res. Oceans **93**: 10749–10768. doi:10.1029/JC093iC09p10749

Morel, A., and S. Maritorena. 2001. Bio-optical properties of oceanic waters: A reappraisal. J. Geophys. Res. Oceans **106**: 7163–7180. doi:10.1029/2000JC000319

Myneni, R. B., C. D. Keeling, C. J. Tucker, G. Asrar, and R. R. Nemani. 1997. Increased plant growth in the northern high latitudes from 1981 to 1991. Nature **386**: 698–702. doi:10.1038/386698a0

Nieminen, M., S. Sarkkola, T. Sallantaus, E. M. Hasselquist, and H. Laudon. 2021. Peatland drainage—A missing link behind increasing TOC concentrations in waters from high latitude forest catchments? Sci. Total Environ. **774**: 145150. doi:10.1016/j.scitotenv.2021.145150

Opdal, A. F., T. Andersen, D.O. Hessen, C. Lindemann and D. L. Aksnes. 2023. Dataset for Tracking freshwater browning and coastal water darkening from boreal forests to the Arctic Ocean. Dryad Dataset. doi:10.5061/dryad.xwdbrv1gq

Opdal, A. F., C. Lindemann, and D. L. Aksnes. 2019. Centennial decline in North Sea water clarity causes strong delay in phytoplankton bloom timing. Glob. Chang. Biol. **25**: 3946–3953. doi:10.1111/gcb.14810

Östlund, L., O. Zackrisson, and A. L. Axelsson. 1997. The history and transformation of a Scandinavian boreal forest landscape since the 19th century. Can. J. For. Res. **27**: 1198–1206. doi:10.1139/x97-070

Romera-Castillo, C., H. Sarmento, X. A. Alvarez-Salgado, J. M. Gasol, and C. Marrase. 2010. Production of chromophoric dissolved organic matter by marine phytoplankton. Limnol. Oceanogr. **55**: 446–454. doi:10.4319/lo.2010.55.1.0446

Sætre, R. 2007, *The Norwegian coastal current—Oceanography and climate*. Tapir Academic Press.

Sandén, P., and B. Håkansson. 1996. Long-term trends in Secchi depth in the Baltic Sea. Limnol. Oceanogr. **41**: 346–351. doi:10.4319/lo.1996.41.2.0346

Sholkovitz, E. R. 1976. Flocculation of dissolved organic and inorganic matter during mixing of river water and seawater. Geochim. Cosmochim. Acta **40**: 831–845. doi:10.1016/0016-7037(76)90035-1

Sholkovitz, E. R. 1978. The flocculation of dissolved Fe, Mn, Al, Cu, Ni, Co and Cd during estuarine mixing. Earth Planet. Sci. Lett. **41**: 77–86. doi:10.1016/0012-821X(78)90043-2

Skerlep, M., E. Steiner, A. L. Axelsson, and E. S. Kritzberg. 2020. Afforestation driving long-term surface water browning. Glob. Chang. Biol. **26**: 1390–1399. doi:10.1111/gcb.14891

Thewes, D., E. V. Stanev, and O. Zielinski. 2021. The North Sea light climate: Analysis of observations and numerical simulations. J. Geophys. Res. Oceans **126**: e2021JC017697. doi:10.1029/2021JC017697

Thomas, R. Q., C. D. Canham, K. C. Weathers, and C. L. Goodale. 2010. Increased tree carbon storage in response to nitrogen deposition in the US. Nat. Geosci. **3**: 13–17. doi:10.1038/ngeo721

Thrane, J. E., D. O. Hessen, and T. Andersen. 2014. The absorption of light in lakes: Negative impact of dissolved organic carbon on primary productivity. Ecosystems **17**: 1040–1052. doi:10.1007/s10021-014-9776-2

Timko, S. A., and others. 2015. Depth-dependent photodegradation of marine dissolved organic matter. Front. Mar. Sci. **2**: 66. doi:10.3389/fmars.2015.00066

Tranvik, L. J., and others. 2009. Lakes and reservoirs as regulators of carbon cycling and climate. Limnol. Oceanogr. **54**: 2298–2314. doi:10.4319/lo.2009.54.6_part_2.2298

Turner, J. S., K. A. Fall, and C. T. Friedrichs. 2022. Clarifying water clarity: A call to use metrics best suited to corresponding research and management goals in aquatic ecosystems. Limnol. Oceanogr. Lett. doi:10.1002/lol2.10301

Vähätalo, A. V., and R. G. Wetzel. 2004. Photochemical and microbial decomposition of chromophoric dissolved organic matter during long (months–years) exposures. Mar. Chem. **89**: 313–326. doi:10.1016/j.marchem.2004.03.010

Weyhenmeyer, G. A., Y. T. Prairie, and L. J. Tranvik. 2014. Browning of boreal freshwaters coupled to carbon-iron interactions along the aquatic continuum. PLos One **9**: e88104. doi:10.1371/journal.pone.0088104

Williamson, J. L., and others. 2021. Landscape controls on riverine export of dissolved organic carbon from Great Britain. Biogeochemistry.

Wilson, R. J., and M. R. Heath. 2019. Increasing turbidity in the North Sea during the 20th century due to changing wave climate. Ocean Sci. **15**: 1615–1625. doi:10.5194/os-15-1615-2019

Xiao, Y. H., T. Sara-Aho, H. Hartikainen, and A. V. Vahatalo. 2013. Contribution of ferric iron to light absorption by chromophoric dissolved organic matter. Limnol. Oceanogr. **58**: 653–662. doi:10.4319/lo.2013.58.2.0653

Yamashita, Y., and E. Tanoue. 2004. In situ production of chromophoric dissolved organic matter in coastal environments. Geophys. Res. Lett. **31**: L14302.